(8) Konda, A.; Nose, K.; Ishikawa, H. *J. Polym. Sci., Polym. Phys. Ed.* **1976**, *14*, 1495.
(9) Misra, A.; Stein, R. S. *J. Polym. Sci., Polym. Phys. Ed.* **1979**, *17*, 235.
(10) Bosley, D. E. *J. Appl. Polym. Sci.* **1964**, *8*, 1521.
(11) de Daubeny, R.; Bunn, C. W.; Brown, C. J. *Proc. R. Soc. London, Ser. A* **1954**, *226*, 531.
(12) Roe, R.-J.; Krigbaum, W. R. *J. Chem. Phys.* **1964**, *40*, 2608.
(13) Krigbaum, W. R.; Roe, R.-J. *J. Chem. Phys.* **1964**, *41*, 737.
(14) Roe, R.-J. *J. Appl. Phys.* **1965**, *36*, 2024.
(15) Krigbaum, W. R.; Balta, Y. I. *J. Phys. Chem.* **1967**, *71*, 1770.
(16) Matsuo, M.; Hirota, K.; Fujita, K.; Kawai, H. *Macromolecules* **1978**, *11*, 1000.
(17) Matsuo, M.; Ozaki, F.; Kurita, H.; Sugawara, S.; Ogita, T. *Macromolecules* **1980**, *13*, 1187.
(18) Stein, R. S.; Norris, F. H. *J. Polym. Sci.* **1956**, *21*, 381.
(19) Bunn, C. W.; de Daubeny, R. *Trans. Faraday Soc.* **1954**, *50*, 1173.
(20) Sakaguchi, N.; Oda, T.; Nakai, A.; Kawai, H. *Seni-Gakkaishi* **1977**, *33*, 779.
(21) Samuels, R. J. *J. Polym. Sci., Part C* **1966**, *13*, 37.
(22) van Aartsen, J. J.; Stein, R. S. *J. Polym. Sci., Part A-2* **1971**, *9*, 295.
(23) Motegi, M.; Oda, T.; Moritani, M.; Kawai, H. *Polym. J.* **1970**, *1*, 209.
(24) Picot, C.; Stein, R. S.; Motegi, M.; Kawai, H. *J. Polym. Sci., Part A-2* **1970**, *8*, 2115.
(25) Hashimoto, T.; Todo, A.; Kawai, H. *Polym. J.* **1978**, *10*, 521.
(26) Hoseman, R.; Bagchi, S. N. "Direct Analysis of Diffraction by Matter"; North-Holland Publishing Co.: Amsterdam, 1962.
(27) Hashimoto, T.; Todo, A.; Murakami, Y.; Kawai, H. *J. Polym. Sci., Polym. Phys. Ed.* **1977**, *15*, 501.
(28) Clough, S.; van Aartsen, J. J.; Stein, R. S. *J. Appl. Phys.* **1965**, *36*, 3072.
(29) Hashimoto, T.; Nagatoshi, K.; Todo, A.; Hasegawa, H.; Kawai, H. *Macromolecules* **1974**, *7*, 364.

# Oriented Crystallization of Poly(ethylene terephthalate) under Uniaxial Stretching

**Takako Terada,† Chie Sawatari, Toyoko Chigono, and Masaru Matsuo***

*Department of Clothing Science, Faculty of Home Economics, Nara Women's University, Nara 630, Japan.* *Received February 24, 1982*

ABSTRACT: The deformation behavior of poly(ethylene terephthalate) films was investigated in terms of orientation of the amorphous chain segments and deformation of superstructures by using small-angle light scattering and birefringence techniques. The elongation was done in a hot air oven and in a hot water bath at different temperatures. The orientation of the amorphous chain segments increased considerably with decreasing elongation temperature. From this it is concluded that the mobility of the polymer chains increases with increasing temperature and, therefore, the amorphous regions stretched at lower temperature behave like paracrystallites. This phenomenon was well accounted for by the results calculated on the basis of a model proposed by Roe and Krigbaum concerning the orientation distribution of statistical segments in deformed networks. Differential scanning calorimetry experimental results supported the temperature dependence of the mobility of the polymer chains. Light scattering patterns at lower extension ratios showed four-leaf lobes extended in the direction of stretching having a maximum in the polar direction along the azimuthal angle of highest intensity. With increasing extension ratios, the scattering exhibited multilobed patterns having sharp narrow four-leaf streaks in addition to the lobes. The appearance of the streak depended on the crystallinity of the film, which is affected by the elongation temperature. These results indicate that the orientation and deformation of sheaflike textures are associated with oriented crystallization. In addition, the shrinkage of bulk specimens was profoundly affected by the crystallinity.

## Introduction

In the previous paper,[1] the deformation mechanism of poly(ethylene terephthalate) (PET) was investigated both theoretically and experimentally in terms of the molecular orientation and superstructural deformation by means of small-angle light scattering, X-ray diffraction, and birefringence techniques. These studies showed that the deformation mechanism is affected by the crystallinity of the undrawn specimens. When an undrawn film with a high degree of crystallinity (about 43% crystallinity) was stretched, the specimen showed almost a constant value of crystallinity under uniaxial stretching; the $H_v$ light scattering pattern had four lobes extended in the horizontal direction and showed a maximum in the polar direction along the azimuthal angle of highest intensity. The deformation was therefore accounted for by a spherulitic model with an affine deformation. On the other hand, when an amorphous film (about 3% crystallinity) was stretched, the crystallinity increased with increasing extension ratio. The $H_v$ scattering showed a broad four-leaf lobe pattern at small azimuthal angles and a sharp narrow four-leaf streak pattern at large azimuthal angles. The analysis was carried out by comparing the theoretical and observed patterns. The agreement between the calculated and observed patterns suggested the occurrence of crystallization associated with the existence of row-nucleated sheaflike textures whose rows are preferentially oriented at a particular angle with respect to the stretching direction.

In order to provide more conclusive evidence about the oriented crystallization, we investigated the deformation of the amorphous PET film in terms of the relation between crystallinity and scattering pattern as well as in terms of the relation between the shape of differential scanning calorimetry (DSC) curves and the second-order orientation factor of the amorphous chain segments. The investigation was further extended to shrinkage mechanisms of bulk specimens.

## Experimental Section

Samples were prepared from 385-$\mu$m amorphous PET films obtained through the courtesy of the Film Division of Toray Industries, Inc., Siga. The density of these films measured by a pycnometer, with *n*-heptane–carbon tetrachloride as a medium, was found to be 1.338 g/cm$^3$. Elongation was done under two

† Present address: Tamaki Women's College.

0024-9297/82/2215-0998$01.25/0 

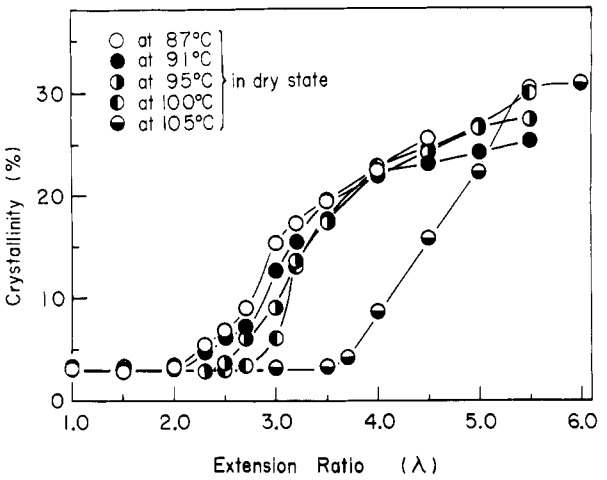


**Figure 1.** Crystallinity vs. extension ratio for PET stretched at five temperatures between 87 and 105 °C in a dry atmosphere.

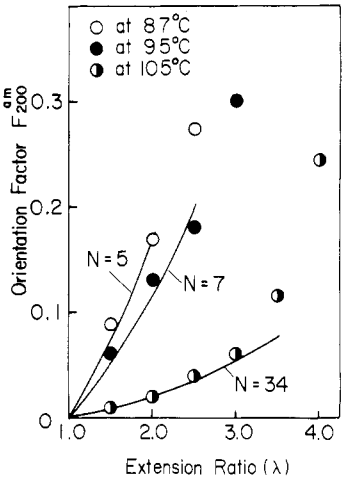


**Figure 2.** Experimental and theoretical results for the second-order orientation factor $F_{200}^{am}$ of the amorphous chain segments for PET stretched at 87, 95, and 105 °C in a dry atmosphere. The points correspond to the experimental data while the curves are calculated.

conditions, namely, in a hot air oven and in a hot water bath. In the case of the hot air oven, the specimen was preheated for 15 min at five temperatures between 87 and 105 °C, all above the glass transition temperature. Immediately following the end of the stretching, the stretcher with the sample was quenched to room temperature. The sample was removed from the stretcher after 10 min. The lowest temperature at which the PET film used in this experiment could be stretched without necking was 87 °C. In the case of the hot water bath, each specimen was held at two temperatures, namely, 65 and 80 °C; these temperatures are above and below $T_g$, respectively. In spite of the different elongation temperatures, the two specimens retained the amorphous state of the film and were elongated without necking up to the desired extension ratios. After the stretching, the quenching was carried out in accordance with the procedure of the former case.

Weight percentage crystallinity was calculated by assuming the densities of the crystal and amorphous regions to be 1.455 and 1.335 g/cm$^3$,[2] respectively. The second-order orientation factor of the amorphous chain segments was calculated from the birefringence of drawn specimens with crystallinities of less than 10% in order to neglect the birefringence of the crystalline phase.

The thermal behavior of PET was studied with a Rigaku differential scanning calorimeter (8089 TG-DSC). Each film was cut into identical circular shapes weighing 16 mg, and the samples were placed in a standard aluminum sample pan. Samples were heated at a constant rate of 10 °C/min. Since the shape of the DSC traces and the location of the peak for a given heating rate are very dependent on the packing, geometry, and size of the specimen, great care was taken to keep these parameters as constant as possible.

Light scattering patterns were obtained with a 3-mW He–Ne gas laser as a light source. Diffuse surfaces were avoided by sandwiching the specimens between microcover glasses with silicone oil of an appropriate refractive index as an immersion fluid.

## Results and Discussion

Figure 1 shows crystallinity as a function of extension ratio for specimens stretched at several temperatures between 87 and 105 °C. The crystallinity shows an almost constant value (about 3%) at extension ratios below $\lambda$ = 2.0, above which it shows a sharp increase as the elongation temperature is decreased. The value of $\lambda$ where the crystallinity increases becomes smaller. This indicates that extensive strain-induced crystallization takes place even at temperatures as low as 87 °C. However, when drawn samples were held with fixed dimensions for 300 min at temperatures between 87 and 105 °C, the crystallinity was found to increase in proportion to the increase of the treatment temperature. This increase in crystallinity is thought to be due to the effect of thermal crystallization and this tendency is in contrast with that of the oriented crystallization discussed in Figure 1.

Figure 2 shows the experimental and theoretical results for the second-order orientation factor $F_{200}^{am}$ of the amorphous chain segments. The experimental orientation factors of specimens stretched at 87 and 95 °C show a considerable increase while that at 105 °C shows only a gradual increase; this indicates that the orientation of the amorphous chain segments is temperature dependent even at extension ratios below $\lambda$ = 2.0, the effect being independent of the increase in crystallinity shown in Figure 1. That is, higher orientation can be produced as the elongation temperature becomes lower. In order to analyze this mechanism qualitatively, we calculated the orientation factors of the amorphous chain segments by using a method proposed by Roe and Krigbaum[3] to estimate the orientation distribution function of statistical segments in deformed networks of completely amorphous cross-linked polymers. Although the method has obvious limitations in applications to crystallizing linear polymers, it was successfully used by Krigbaum and Taga[4] to estimate the orientation of the remaining amorphous chains during the crystallization of isotactic polystyrene. The method should be applicable in the case of the deformation of the PET sample with 3% crystallinity, if we assume that crystallites are effectively cross-links causing the specimens to behave like an amorphous cross-linked network.

According to Roe and Krigbaum,[3] the orientation distribution function may be given as a series of Legendre polynomials, i.e.

$$\omega(\xi) = \sum_{l=0}^{\infty} \omega_l \Pi_l(\xi) \qquad (l \text{ even}) \tag{1}$$

where $\xi = \cos\chi$ and $\chi$ is the angle between a statistical segment and the stretching direction. $\Pi_l(\xi)$ is the normalized Legendre function and $\omega_l$ is a coefficient that was given by a series expansion of the distribution function.[3] In the case of $l$ = 2

$$2\pi\left(\frac{2}{5}\right)^{1/2}\omega_2 = F_{200}^{am} = \int_{-1}^{1}\omega(\xi)\frac{3\xi^2-1}{2}\,d\xi = \frac{1}{5N}\left(\lambda^2 - \frac{1}{\lambda}\right) + \frac{36}{875N^2}\left(\lambda^4 + \frac{\lambda}{3} - \frac{4}{3\lambda^2}\right) + \frac{108}{6125N^3}\left(\lambda^6 + \frac{3\lambda^3}{5} - \frac{8}{5\lambda^3}\right) \tag{2}$$

where $N$ is the number of freely jointed statistical segments of a drawn sample. The values of $N$ in Figure 2 were adopted to give the best fit between the experimental and

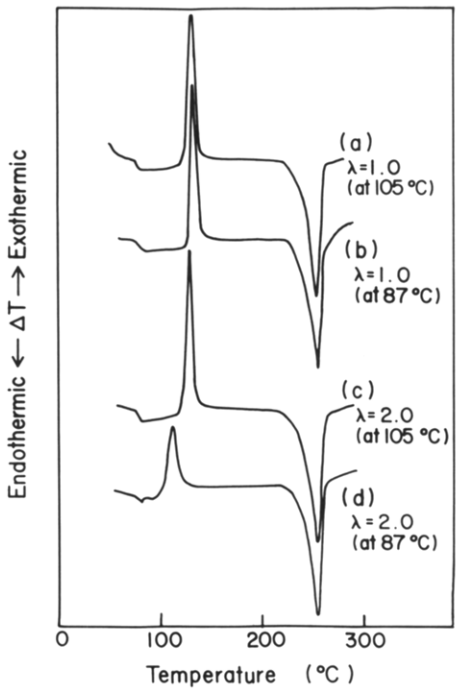


**Figure 3.** DSC curves of PET films: (a) undrawn sample heated at 105 °C; (b) undrawn sample heated at 87 °C; (c) sample stretched to λ = 2.0 at 105 °C; (d) sample stretched to λ = 2.0 at 87 °C.

theoretical curves. The value of $N$ corresponding to the best fit remains constant at each temperature during the deformation. $N$ increases with increasing elongation temperature, which suggests that the orientation behavior of the amorphous chain segments at 105 °C is somewhat different from that at 95 and 87 °C. It would be expected that the mobility of polymer chains increases with increasing temperature and, therefore, the amorphous regions of the specimen stretched at lower temperature behave somewhat like paracrystallites. The DSC data sensitively reflect this characteristic orientation behavior.

Figure 3 presents DSC data, in which curves a and b correspond to the unstretched specimens preheated for 15 min at 105 and 87 °C, respectively, while curves c and d correspond to the specimen stretched to λ = 2.0 at 105 and 87 °C, respectively, after preheating. For curves a–d, each melting endotherm appears around 257 °C, independent of the heat treatment and elongation temperature. By contrast, the position and shape of the crystallizing exotherms depend on the sample preparation conditions. The exotherm of curve a is less intense than that of curve b, which is presumably due to a small thermal crystallization effect. On the other hand, the exotherm of curve d is less sharp than that of curve c. This indicates that the amorphous regions behave somewhat like paracrystallites when the specimen is stretched at temperatures close to $T_g$. This is obviously due to the effect of oriented crystallization and this effect predominates over the effect of thermal crystallization in the case of the drawn sample. Therefore, the DSC measurements have the advantage of revealing small changes of crystallinity that are impossible to detect on the basis of the density measured by pycnometry. The superstructures that developed in the oriented amorphous samples were investigated by $H_v$ light scattering. It was possible to obtain scattering patterns from samples that showed little or no crystallinity and for which no superstructure could be observed under the microscope.

Figure 4 shows $H_v$ scattering patterns for samples stretched up to λ = 2.0. All the patterns have scattering

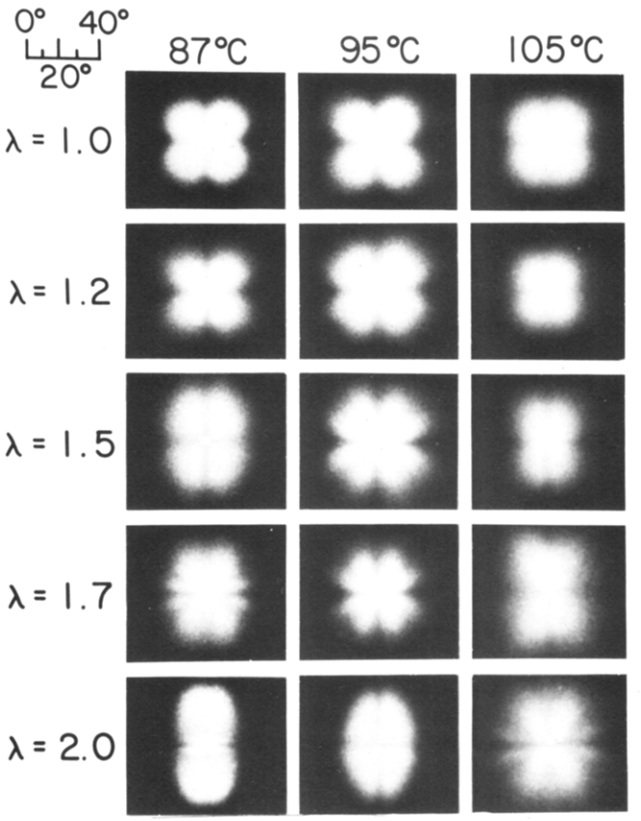


**Figure 4.** $H_v$ scattering patterns for PET stretched to an extension ratio of λ = 2.0 in a dry atmosphere.

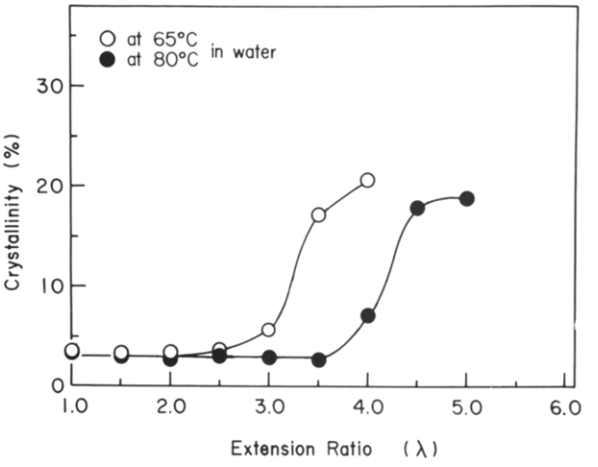


**Figure 5.** Crystallinity vs. extension ratio for PET stretched in water baths at 65 and 80 °C.

lobes with maxima in intensity along the scattering angle direction, and the lobes are inclined toward the scattering direction. Such patterns are characteristic of scattering from sheaflike textures whose sheaf axes are oriented preferentially in the direction normal to stretching.[2] Although the crystallinities of the specimens have the same value, the scattering patterns show a dependence on the elongation temperature. This suggests that it is the increase of the orientation factor $F_{200}^{am}$ that influences the change in the scattering pattern. An experiment similar to that of Figure 4 was carried out by Misra and Stein.[5] According to their data for samples stretched at 80 °C, the patterns showed scattering from rodlike textures at lower elongations up to λ = 1.8, whereas the patterns with extension ratios from λ = 2.15 to λ = 3.15 had four lobes oriented in the stretching direction and showed a maximum intensity in each lobe. This phenomenon is quite

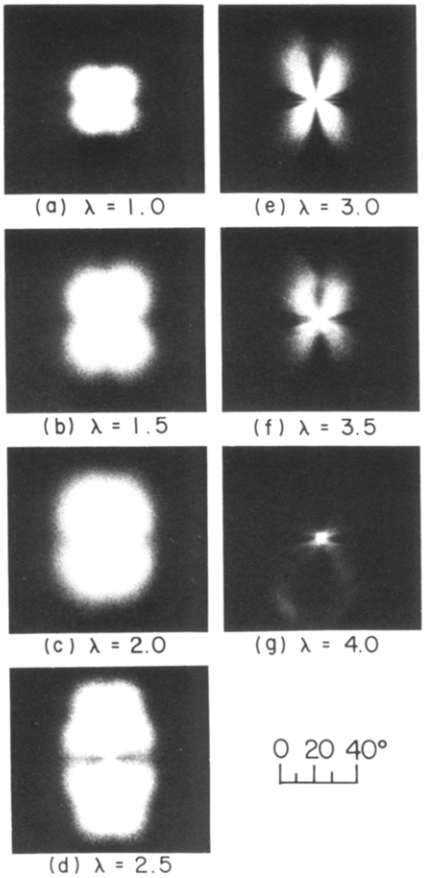


**Figure 6.** $H_v$ scattering patterns for PET stretched in 65 °C water.

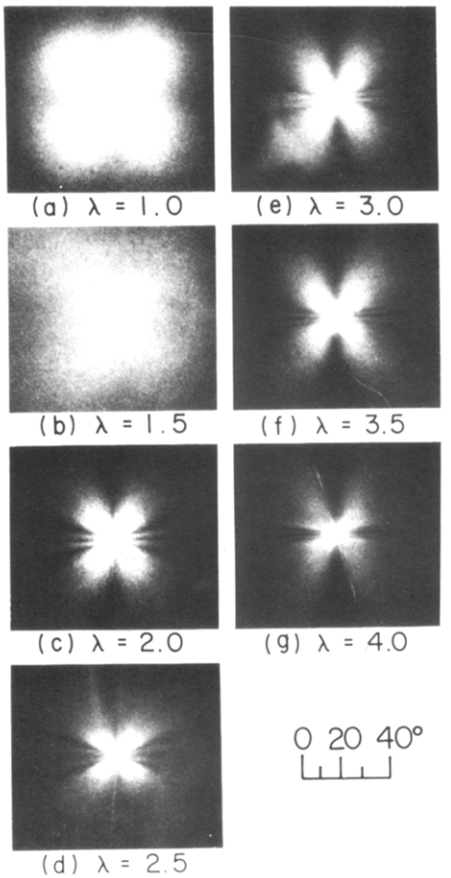


**Figure 7.** $H_v$ scattering patterns from drawn PET films held with fixed dimensions for 15 min in a 100 °C water bath. Elongations were carried out under the same experimental conditions as those in Figure 5.

different from the results for samples stretched at 87 °C in Figure 4. Scattering from rodlike textures cannot be observed and the patterns up to $\lambda = 1.7$ are eight-lobed such as already observed in the previous paper.[1]

We now discuss the oriented crystallization of PET films in a hot water bath. Figure 5 shows the change in crystallinity with increasing extension ratio for the specimens stretched at 65 and 80 °C. An increase in crystallinity was observed up to $\lambda = 3.0$ for the specimen stretched at 65 °C and up to $\lambda = 3.5$ for that at 80 °C; this is similar to the case when the specimen was stretched in a hot air oven.[1] The results in Figures 1 and 5 indicate that crystallinity increases gradually when the stretching conditions are such that the polymer chains are mobile so that the strain relaxes. On the other hand, a considerable increase in the stretching conditions is required to produce a decrease in chain mobility and then the strain does not relax with further increases of $\lambda$.

Figure 6 shows a series of $H_v$ scattering patterns for samples stretched in a water bath at 65 °C. The four-leaf lobes of all the patterns were extended in the direction normal to stretching, and there is a maximum in the polar direction along the azimuthal angle of highest intensity. Moreover, the pattern beyond $\lambda = 3.0$, which is associated with an increase in crystallinity, exhibited sharp narrow four-leaf streaks in addition to the lobes. The change in the shape of the scattering pattern with increasing $\lambda$ is similar to that observed for the specimen stretched in a hot air oven at 95 °C in the previous paper.[1] Therefore the oriented crystallization of PET films in the water bath and in an oven is presumed to be essentially the same, despite the difference in the treatment temperatures. According to the theoretical analysis in the previous paper,[1] these observations indicate that the scattering arises from sheaflike superstructures resulting from lamellar overgrowth associated with rows of nucleating points and subsequent lamellar branching that occurs predominantly perpendicular to the stretching direction. Moreover, the sharp narrow streaks shown in patterns d, e, and f would be attributed to the interference effect of scattering from the assemblies of the sheaflike textures.

Figure 7 shows a series of scattering patterns from the drawn specimens after treatment at fixed dimensions for 15 min in a water bath at 100 °C. The drawn specimens were prepared under the same conditions as discussed in Figure 6. The patterns below $\lambda = 1.5$ are more diffuse and show larger lobes than the corresponding patterns in Figure 6. All of the patterns beyond $\lambda = 2.0$ have four lobes and four streaks. The lobes show no indication of the intensity maxima along the scattering angle. The intensity is the greatest in the center and decreases monotonically with increasing scattering angle. The lobes are inclined toward the stretching direction. These observations are indicative of scattering from rods oriented predominantly perpendicular to the stretching direction. This texture is probably due to the fact that the sheaflike morphology, the long axis being oriented normal to the stretching direction, changes into a fibrillar morphology as a result of surface tension effects that result when the specimen is constrained to fixed dimensions during annealing. The fact that the tension is an important factor for the formation of rodlike textures is consistent with the result reported by Misra and Stein.[5] In their report,[5] rodlike textures were observed in a cold-drawn sample annealed at a constant length at 140 °C for 10 min. Returning to Figure 7, we observe sharp narrow streaks in patterns c and d. They appear only during the annealing

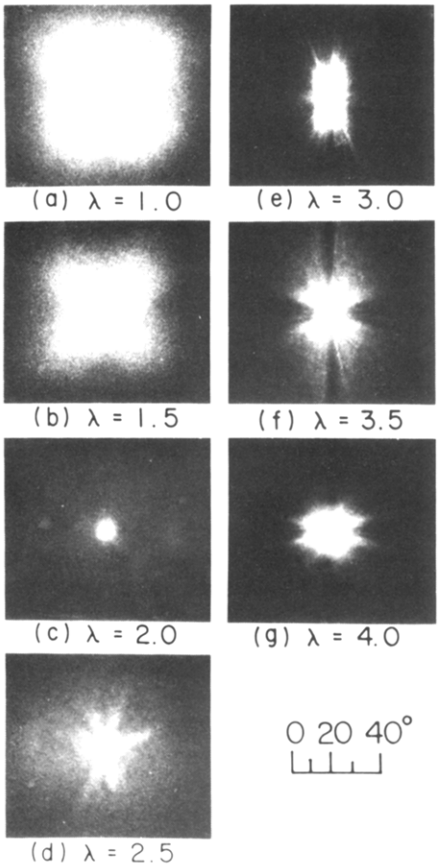


**Figure 8.** $H_v$ scattering patterns from drawn PET films held with unconstrained dimensions for 15 min in a 100 °C water bath. Elongations were carried out under the same experimental conditions as those in Figure 5.

of drawn samples with fixed dimensions. The appearance of the sharp streaks is thought to be due to an interference effect arising from the scattering of an assembly of rodlike textures. This interference effect becomes more pronounced when the sheaflike texture is transformed into a rodlike texture by annealing, and the effect is dependent upon the increase of crystallinity. The crystallinity of the drawn specimens beyond λ = 2.0 reaches about 33% through the annealing.

Figure 8 shows a series of $H_v$ scattering patterns for drawn samples held with unconstrained dimensions for 15 min in a water bath at 100 °C. The drawn specimens shrank in the hot water. The scattered intensity for the drawn specimen with λ = 2.0, which showed the greatest shrinkage, becomes almost zero and it is only apparent at the center of the pattern. This seems to be due to the random orientation of the optical scattering elements with respect to the radial direction of the sheaflike texture. That is, although a spherulitic array of the scattering elements surrounded by the medium retains a sort of ordered orientation distribution with respect to the radius under uniaxial stretching, the oriented elements assume a random orientation mode during the shrinkage process. In addition, the birefringence of the specimen showing patterns c and d was almost zero. Pattern e has a novel shape, which is presumably produced by the very complicated deformation mechanism of sheaflike textures during shrinkage. Patterns f and g are somewhat indistinct but maintain the four-leaf lobes and streaks. This indicates that randomization of the scattering elements as well as destruction of the superstructure for the drawn specimens becomes less effective as λ increases beyond 3.5. When a specimen that had been stretched beyond λ = 3.5 is allowed to shrink, the change in birefringence is found to decrease with increasing λ.

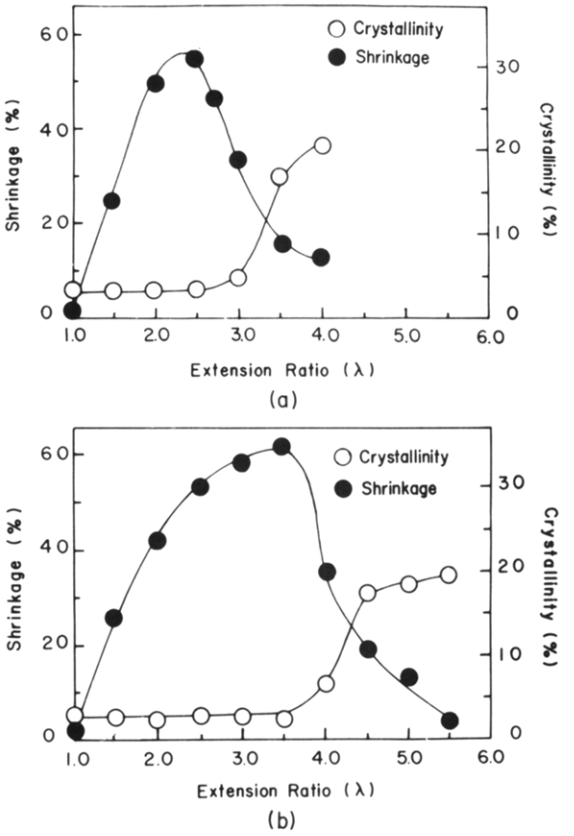


**Figure 9.** Crystallinity and shrinkage of bulk specimens as a function of extension ratio.

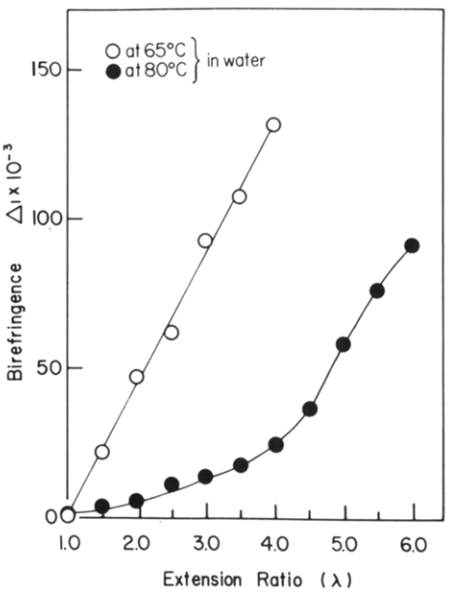


**Figure 10.** Birefringence vs. extension ratio for PET films stretched in water baths at 65 and 80 °C.

Figure 9 shows the crystallinity and shrinkage of bulk specimens as a function of λ; experiments a and b were carried out with the specimens stretched at 65 and 80 °C, respectively. The shrinkage increases in both cases and passes through a maximum at a value of λ where the crystallinity begins to increase. That is, the maxima in the shrinkage ratios occur at λ = 2.5 at 65 °C and at λ = 3.5 at 80 °C. Beyond the maxima the shrinkage ratios tend to decrease with increasing crystallinity; this is associated with the fact that as the crystallinity increases, the crys-

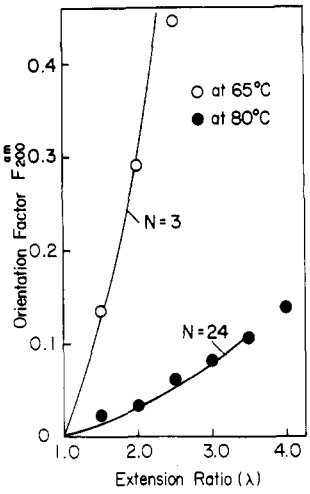


**Figure 11.** Experimental and theoretical results for the second-order orientation factor $F_{200}^{am}$ of the amorphous chain segments for PET films stretched in water baths at 65 and 80 °C. The points correspond to the experimental data while the curves are calculated.

tallites acting as cross-links prevent the amorphous chain segments from assuming a random coil configuration during shrinkage.

Figure 10 shows the change in birefringence with increasing λ. The birefringence of specimens stretched in the 65 °C water bath shows a considerable linear increase that is independent of an increase in crystallinity. On the other hand, the birefringence of specimens stretched in the 80 °C water bath increases slowly up to λ = 3.5. This contrasting behavior is close to the mobility of the polymer chains under stretching. When the specimen is stretched below $T_g$, the strain increases considerably and does not relax with further increases of λ; this implies a considerable orientation of the polymer chains. By contrast, when the specimen is stretched above $T_g$, the strain that occurs during elongation relaxes easily, so that there is a gradual increase in the orientation of the polymer chains. Returning to Figure 10, we see that there is a considerable increase in birefringence when the sample at 80 °C is stretched beyond λ = 4.0. This is thought to be due to oriented crystallization and is obviously related to the preferential orientation of the crystal *c* axes in the direction of stretching.

Figure 11 shows experimental and theoretical results for the second-order orientation factor of the amorphous chain segments calculated from the birefringence data in Figure 10. The experimental result at 65 °C shows a considerable increase, while that at 80 °C is less pronounced. The theoretical calculations of the method of Roe and Krigbaum[3] are limited to the case of crystallinity less than 3%. The values of $N$ corresponding to the best fit are constant and independent of λ at each temperature. Stretching below $T_g$ requires that $N = 3$ for the best fit, which indicates that below $T_g$ the amorphous regions behave as paracrystallites.

Figure 12 shows DSC curves of the drawn samples; curves a and b correspond to λ = 1.5 at 80 and 65 °C, respectively, while curves c and d correspond to λ = 2.0 at 80 and 65 °C, respectively. The position and shape of crystallizing exotherms are affected by the elongation temperature. The profile of the four curves indicates that the amorphous regions stretched below $T_g$ behave like paracrystallites while for stretching above $T_g$, the amorphous regions exhibit an active mobility of polymer chains and require a considerable energy to crystallize. This tendency is similar to the results shown in Figure 3.

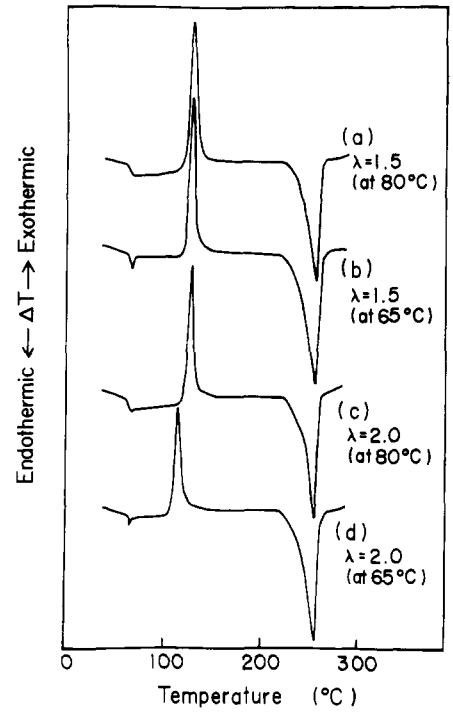


**Figure 12.** DSC curves of PET films stretched in a hot water bath: (a) sample stretched to λ = 1.5 at 80 °C; (b) sample stretched to λ = 1.5 at 65 °C; (c) sample stretched to λ = 2.0 at 80 °C; (d) sample stretched to λ = 2.0 at 65 °C.

## Conclusion

This paper is concerned with the study of the orientation of the amorphous chain segments and the deformation mechanism of superstructures in PET films under uniaxial stretching. The elongation was carried out in two ways, namely, in a hot air oven at five temperatures between 87 and 105 °C and in a hot water bath at 65 and 80 °C.

(i) When the specimen was stretched in a hot air oven, the second-order orientation factor of the amorphous chain segments was found to decrease with increasing elongation temperature. This behavior was well accounted for by calculations based on a model proposed by Roe and Krigbaum[3] concerning the orientation distribution function of statistical segments in deformed polymer networks. The results indicated that the number of connected statistical segments decreases with decreasing elongation temperature. This would be expected if the mobility of the segments increases with temperature so that the strain relaxes faster. This was supported by DSC measurements.

(ii) For the specimens stretched in a hot water bath, the orientation of the amorphous chain segments was also estimated in terms of the second-order orientation factor by the same method used in the former case. The result indicated that the amorphous regions of samples drawn below $T_g$ (65 °C) behave like paracrystallites, while for specimens drawn above $T_g$ (80 °C), the amorphous regions exhibit active mobility of polymer chains.

The $H_v$ scattering patterns for the specimens stretched at 65 °C had four-leaf lobes with a maximum in the polar direction along the azimuthal angle of the highest intensity and were extended in the direction normal to stretching. This type of pattern is characteristic of scattering from sheaflike textures whose long axis is oriented preferentially in the direction normal to stretching. The patterns for the samples stretched beyond λ = 3.0 exhibited sharp narrow four-leaf streaks in addition to the lobes, and such patterns could be attributed to the interference effect of scattering from assemblies of sheaflike textures. When constrained drawn samples were put into a hot water bath at 100 °C,

the intensity of the lobes was greatest in the center and decreased monotonically with increasing scattering angle. This is indicative of a transformation from sheaflike to rodlike textures having a fibrillar morphology. This transformation was postulated to depend on surface tension effects resulting from restriction of the shrinkage of the drawn specimen during annealing. A similar result was reported by Misra and Stein.[5] When unconstrained drawn specimens were put into a hot water bath at 100 °C, they shrank. The degree of shrinkage of bulk specimens decreased with increasing crystallinity of the drawn specimens before annealing. This tendency was related to obstruction of the randomization of amorphous chain segments by the crystallites during the relaxation process. This suggests that there is an increase in the number of cross-linking points of the amorphous chain segments, leading to an increase of crystallinity.

**Acknowledgment.** We thank Professor Kawai, Department of Polymer Chemistry, Faculty of Engineering, Kyoto University, Japan, for valuable comments and suggestions. Thanks are also due to Dr. Inoue and Mr. Motegi, Toray Industries, Inc., Siga, for the sample used and for helpful comments. We are also grateful to Dr. R. St. John Manley, Department of Chemistry, McGill University, for his kind help with the English presentation.

## References and Notes

(1) Matsuo, M.; Tamada, M.; Terada, T.; Sawatari, C.; Niwa, M. *Macromolecules*, preceding paper in this issue.
(2) de Daubeny, R.; Bunn, C. W.; Brown, C. J. *Proc. R. Soc. London, Ser. A* **1954**, *226*, 531.
(3) Roe, R.-J.; Krigbaum, W. R. *J. Appl. Phys.* **1964**, *35*, 2215.
(4) Krigbaum, W. R.; Taga, T. *J. Polym. Sci., Polym. Phys. Ed.* **1979**, *17*, 393.
(5) Misra, A.; Stein, R. S. *J. Polym. Sci., Polym. Phys. Ed.* **1979**, *17*, 235.

# Crystallization of the Extended Conformation from the Bulk in Solvent-Exposed Films of Isotactic Polystyrene

**Pudupadi R. Sundararajan* and Nancy J. Tyrer**

*Xerox Research Centre of Canada, 2480 Dunwin Drive, Mississauga, Ontario L5L 1J9, Canada.* *Received December 16, 1981*

ABSTRACT: The extended conformation, with a nonstaggered tt state of skeletal bonds, occurs in gels of isotactic polystyrene (iPS). Intramolecular interaction between adjacent phenyls is predominant in this conformation. Although gels containing the extended conformation melt in the range 80–120 °C, this conformation cannot be crystallized from the bulk by annealing below $T_m$. It is shown that solvent molecules are required to provide the intermolecular interaction necessary for crystallization. Thus, through exposure of amorphous films of iPS to bulky hydrocarbon or substituted aromatic solvent vapor, crystallization of the extended conformation from the bulk has been achieved at room temperature. A unit cell with $a$ = 21.0, $b$ = 16.4, and $c$ = 30.6 Å containing four chains and 8–16 solvent molecules has been proposed. The extended conformation can be induced by solvent exposure even in semicrystalline films already containing the threefold helical structure. Thus, it is shown that the extended conformation exists with significant perpetuation in the amorphous zones of semicrystalline films containing the threefold helical structure. Scanning electron micrographs show that the extended conformation, when crystallized, forms dendritic structures. It is suggested that the lower $T_m$ of this structure compared to that of the threefold helical structure is due not to intramolecular instability but rather to the requirement of the presence of solvent molecules in the lattice.

## Introduction

Conformational energy calculations on isotactic polystyrene (iPS) have shown[1] that conformations near the tt state of adjacent skeletal bonds are not forbidden as heretofore believed. Although the perfectly staggered tt state with $(\phi_i, \phi_{i+1}) = (0°, 0°)$ ($\phi_i$ and $\phi_{i+1}$ being the rotations defining the conformations around the skeletal bonds $i$ and $i + 1$) incurs severe overlap of adjacent phenyl groups, rotations of about 20° in $\phi_i$ and $\phi_{i+1}$ relieves such an overlap and the energy of the nonstaggered tt state becomes comparable to that of the gt state (which, when perpetuated, generates the familiar threefold helix with a repeat distance of 6.6 Å found in the crystalline state[2]). This feature was found to be common for most isotactic vinyl chains[3,4] bearing planar substituents, for example, for poly(methyl methacrylate), poly(α-methylstyrene), poly(vinyl acetate), and poly(*N*-vinylcarbazole).

The presence of the nonstaggered tt conformation of successive skeletal bonds is required to construct the double-helical structure proposed by Kusanagi et al.[5] for isotactic PMMA. The X-ray diffraction pattern obtained by Atkins et al.[6] for isotactic polystyrene gels prepared by quenching the solution in decalin was different from that of the crystalline threefold helical structure. The interim solution that they offered on the basis of a syncephalic (head-to-head, tail-to-tail) sequence along the chain was contradicted by their $^{13}C$ NMR data. However, our calculations[1] reported in 1979 showed that the X-ray diffraction pattern from iPS gels can be interpreted by using the nonstaggered tt conformation of skeletal bonds in terms of an isotactic chain containing 12 monomers in a repeat distance of 30.6 Å. (This will be referred to as the extended conformation hereafter). In this conformation, the rise per repeat unit along the helix is 2.55 Å, which is larger than the distance between successive $C^\alpha$ atoms, if tetrahedral bond angles are taken. Enlargement of the angle at the $C^\alpha$ atom to 114° and that at the methylene carbon to 117.8° was necessary to minimize the energy and account for the helix parameters. This was discussed in a previous paper.[1] The calculations[1] also showed that the energy of the extended conformation is lower than that of the threefold helical conformation by about 1 kcal·mol$^{-1}$. Calculations reported later by other authors[7-9] have confirmed the possibility of such an extended conformation for iPS.

Our recent studies[10] on the gelation of iPS, using several types of solvents, showed that although the gels can be obtained from several solvents, the resultant conformation of the chain depends on the stereochemistry and size of the solvent molecule. It was found that with bulky, non-

0024-9297/82/2215-1004$01.25/0 